HHS Public Access

Author manuscript

Clin Cancer Res. Author manuscript; available in PMC 2021 September 01.

Published in final edited form as:

Clin Cancer Res. 2021 March 01; 27(5): 1316–1328. doi:10.1158/1078-0432.CCR-20-3208.

A Performance Comparison of Commonly Used Assays to Detect RET Fusions

Soo-Ryum Yang, M.D.[*,1], **Umut Aypar, Ph.D.**[1], **Ezra Y. Rosen, M.D., Ph.D.**[2], **Douglas A. Mata, M.D., M.P.H.**[1], **Ryma Benayed, Ph.D.**[1], **Kerry Mullaney**[1], **Gowtham Jayakumaran, M.S.**[1], **Yanming Zhang, M.D.**[1], **Denise Frosina**[1], **Alexander Drilon, M.D.**[2], **Marc Ladanyi, M.D.**[1], **Achim Jungbluth, M.D.**[1], **Natasha Rekhtman, M.D., Ph.D.**[1], **Jaclyn F. Hechtman, M.D.**[1]

[1]Department of Pathology, Memorial Sloan Kettering Cancer Center

[2]Department of Medicine, Memorial Sloan Kettering Cancer Center

Abstract

Purpose: Selpercatinib and pralsetinib induce deep and durable responses in advanced *RET* fusion-positive lung and thyroid cancer patients. *RET* fusion testing strategies with rapid and reliable results are critical given recent FDA approval. Here, we assess various clinical assays in a large pan-cancer cohort.

Experimental Design: Tumors underwent DNA-based next generation sequencing (NGS) with reflex to RNA-based NGS if no mitogenic driver or if a *RET* structural variant of unknown significance (SVUS) were present. Canonical DNA-level *RET* fusions and RNA-confirmed *RET* fusions were considered true fusions. Break-apart fluorescence in situ hybridization (FISH) and immunohistochemistry (IHC) performance were assessed in subgroups.

Results: 171 of 41,869 patients with DNA NGS harbored *RET* structural variants, including 139 canonical fusions and 32 SVUS. 12/32 (37.5%) SVUS were transcribed into RNA-level fusions, resulting in 151 oncogenic *RET* fusions. The most common *RET* fusion-positive tumor types were lung (65.6%) and thyroid (23.2%). The most common partners were *KIF5B* (45%), *CCDC6* (29.1%), and *NCOA4* (13.3%). DNA NGS showed 100% (46/46) sensitivity and 99.6% (4459/4479) specificity. FISH showed 91.7% (44/48) sensitivity, with lower sensitivity for *NCOA4-RET* (66.7%, 8/12). 87.5% (7/8) of *RET* SVUS negative for RNA-level fusions demonstrated rearrangement by FISH. The sensitivity of IHC varied by fusion partner: *KIF5B* sensitivity was highest (100%, 31/31), followed by *CCDC6* (88.9%, 16/18) and *NCOA4* (50%, 6/12). Specificity of RET IHC was 82% (73/89).

Conclusions: While DNA sequencing has high sensitivity and specificity, RNA sequencing of *RET* SVUS is necessary. Both FISH and IHC demonstrated lower sensitivity for *NCOA4-RET* fusions.

Keywords

RET; targeted therapy; biomarkers; gene fusions; molecular diagnostics

[*]Corresponding author: [yangs2@mskcc.org], Address: 1275 York Ave, New York, NY 10065, Phone: [212.717.3515].

Introduction

Fusions involving the RET receptor tyrosine kinase (RTK) are recurrent drivers in cancer(1). The RET protein, encoded by the *RET* (REarranged during Transfection) gene, is activated by neurotrophic factors that induce receptor dimerization, phosphorylation of the kinase domain, and signal transduction of downstream pathways in physiologic conditions (2,3). In tumors with activating *RET* fusions, a partner gene, most commonly *KIF5B, CCDC6*, or *NCOA4*, is fused to the distal portion of the *RET* gene including the kinase domain (4–9). This chromosomal rearrangement or structural variant (SV) can generate a constitutively active chimeric protein composed of a C-terminal coil-coiled domain and an N-terminal kinase domain.

Since their initial discovery in papillary thyroid cancers, *RET* fusions have been identified in a diverse set of solid tumors at varying frequencies. Most notably, up to 2% of non-small cell lung cancers (NSCLC) and 10% of thyroid cancers can harbor oncogenic *RET* fusions (10). In addition, *RET* fusions have been infrequently reported (<1%) in other common and rare tumors including colorectal cancer, pancreatic cancer, breast cancer, melanoma, soft-tissue sarcoma, salivary duct carcinoma, and ovarian cancer, among others (10–12). Despite their overall rarity, patients with advanced *RET* fusion-positive tumors collectively represent a large, genomically distinct cohort with suboptimal outcomes to conventional chemotherapy, immunotherapy, and multikinase inhibitors (13–16).

Recently, a new generation of highly selective RET tyrosine kinase inhibitors (TKIs) has been developed to target oncogenic *RET* fusions and mutations(17). In clinical trials, these agents, namely selpercatinib and pralsetinib, have demonstrated deep and durable responses in most patients with advanced *RET* fusion-positive tumors (18–21). Given these dramatic results and the recent FDA-approval of selpercatinib and pralsetinib, testing for *RET* fusions is now standard-of-care for patients with advanced NSCLC and thyroid cancer(22). Currently, there are multiple methods for detecting *RET* fusions including fluorescence in situ hybridization (FISH), reverse-transcriptase polymerase chain reaction (RT-PCR), and DNA/RNA-based next-generation sequencing (NGS). In addition, RET immunohistochemistry (IHC) can be used to measure RET protein expression, which may serve as a surrogate marker for *RET* fusions. Despite the growing number of diagnostic assays, the variability in their performance represents a significant challenge for harmonizing *RET* fusion testing. In prior studies, RET IHC has shown poor correlation with *RET* fusion status as determined by RT-PCR and FISH (23,24). However, these reference methods have not been extensively benchmarked against newer NGS-based assays. Furthermore, DNA-based NGS is known to have a limited sensitivity for certain fusions (25–28), and its accuracy for identifying *RET* fusions remains largely unknown. Here, we compare the performance of DNA- and RNA-based NGS, FISH, and IHC and explore the molecular landscape of actionable *RET* fusions in a large pan-cancer cohort.

Materials and Methods

Case selection

After approval from our institutional review board, a retrospective review of the MSK-IMPACT (DNA-based NGS) and MSK-Fusion panel (RNA-based NGS) results from January 1st, 2014 to May 9th, 2020 was performed. MSK-IMPACT and MSK-Fusion as well as break-apart FISH were all performed in CLIA-approved laboratories following standard operating procedures.

DNA sequencing

Genomic DNA was extracted from formalin-fixed, paraffin-embedded tissue and submitted for MSK-IMPACT. MSK-IMPACT is a hybridization capture-based NGS assay that interrogates all exons and select introns of 468 genes to identify mutations, copy number changes, microsatellite instability status, and select structural variants in its current iteration (previous versions interrogated 341 and 410 genes) (29). All three panels covered the entire coding region of *RET* as well as introns 9-11. Introns 7 and 8 were added in the latest panel with 468 genes.

Structural variant detection

DELLY was used to detect structural variants (SV) from MSK-IMPACT as previously described (30). All SV calls involving *RET* were manually reviewed; only the SVs with high-quality paired-end reads (≥2) were included. In tumors with multiple *RET* SVs, the most canonical SV and/or the SV with the highest read support were selected. *RET* SVs were annotated as kinase fusions if they were predicted to form a protein fusion involving (i) a non-*RET* 5' partner gene and (ii) an intact *RET* kinase domain (NM_020975: exons 12-18) in the 3' partner position. Furthermore, *RET* SVs from MSK-IMPACT were classified into two groups. First, *RET* SVs that predicted *RET* kinase fusions with previously described fusion partners were classified as recurrent oncogenic *RET* fusions. This included inversion-mediated *RET* SVs that were reciprocal to known kinase fusions (e.g., *RET-KIF5B* for *KIF5B-RET*). Second, novel and/or atypical SVs were classified as SVs of unknown significance (SVUS) and further characterized by MSK-Fusion (see below). This included (i) SVs that predicted kinase fusions with novel fusion partners, (ii) SVs with partners mapping to intergenic regions, (iii) intragenic *RET* SVs not involving other genes (e.g., deletion of *RET* exons 3-5), and (iv) SVs predicted to form antisense fusions involving two gene transcripts with incompatible orientations. All protein fusions were annotated as out-of-frame, in-frame, and mid-exonic based on output from DELLY. For our study, SVs with mid-exonic breakpoints were annotated as fusions involving the adjacent uninterrupted exon. In patients with multiple tumors that were analyzed using MSK-IMPACT, the results from the initial tumor sample and/or the sample with paired MSK-Fusion testing were used.

Liquid biopsy testing

Circulating tumor cell-free (cfDNA) was sequenced using MSK-ACCESS in a subset of patients in our cohort. MSK-ACCESS is a hybridization capture-based NGS assay that is optimized for detecting select genetic variants using tumor cfDNA from plasma(31). The

assay targets 129 genes and covers *RET* exons 12-19 and introns 7-11. Manta was used for SV calling as previously described(32).

RNA sequencing

Tumors from formalin-fixed paraffin-embedded tissues were tested for RNA-level fusions using MSK-Fusion. MSK-Fusion is a custom RNA-based NGS assay that uses Anchored Multiplex PCR (via the Archer platform) as previously described (28,33). The custom panel covers select exons in 62 genes including *RET* exons 8-13. All fusion transcripts calls were manually reviewed, and only those with a minimum of 5 unique reads as well as 3 unique reads with unique start sites were reported. Tumors tested included: (i) cases with DNA-level SVUS involving kinase genes including *RET*, as detected by MSK-IMPACT, (ii) *de novo* solid tumors lacking MAPK driver alterations on MSK-IMPACT (e.g., lung adenocarcinoma with no mitogenic drivers), and (iii) cases with clinical evidence of progression to a targeted or hormone therapy but lacking a resistance mechanism on MSK-IMPACT (e.g., *EGFR*-mutated lung adenocarcinoma progressing on EGFR TKI but no detectable resistance alteration).

Definition of fusion-positive and negative cases

Cases with *RET* SVs on MSK-IMPACT were placed into 4 groups based on the results from the above testing: (i) group A: *RET* SVs predicted to form recurrent oncogenic *RET* fusions (*RET* kinase domain and a known 5' partner) and therefore not tested with MSK-Fusion, (ii) group B: *RET* SVs predicted to form recurrent oncogenic *RET* fusions that were confirmed on MSK-Fusion, (iii) group C: *RET* SVUS that were transcribed into *RET* fusions on MSK-Fusion, and (iv) group D: *RET* SVUS that did not result in *RET* fusions on MSK-Fusion. Cases from groups A, B, and C were defined as *RET* fusion positive. Cases from group D were considered *RET* fusion negative. For groups B and C, data from RNA sequencing were used for annotating the fusions.

Break-apart FISH

Break-apart fluorescence in situ hybridization (FISH) was performed on a subset of *RET* fusion-positive (n=48) and negative cases (n=25) using a commercial break-apart FISH probe for *RET* (ZytoVison, Bremerhaven, Germany) (Supplementary Methods). For each hybridization, a minimum of 100 non-overlapping nuclei were assessed for numbers of green and red signals. Using a pre-specified cutoff, FISH was considered positive for a *RET* rearrangement if ≥10% tumor cells demonstrated a rearrangement, as defined by the separation of red (5') and green (3') signals ≥2 signal diameter including atypical signal patterns. FISH analysis was performed by qualified clinical cytogenetic technologists and interpreted by a board-certified clinical cytogeneticist (UA).

RET fusion-positive cases were selected from groups A, B, and C where additional material was available. *RET* fusion-negative cases included group D cases (n=8) and treatment-naïve lung adenocarcinomas that were negative for *RET* SVs but positive for other activating MAPK alterations by MSK-IMPACT (n=17). The latter group was included given that *RET* fusions are mutually exclusive with oncogenic drivers in treatment-naïve lung cancers (7).

Immunohistochemistry

RET IHC was performed on 70 *RET* fusion-positive and 89 negative cases using the clone EPR2871 (ab134100; Abcam, Cambridge, MA). EPR2871 is a rabbit recombinant monoclonal antibody generated to a proprietary peptide in the C-terminal portion of RET and has been used in prior studies (8,24) (Supplementary Methods).

RET fusion-positive cases were selected from groups A, B, and C where additional material was available. The negative control cohort included (i) group D cases (n=9), (ii) lung adenocarcinomas (n=34) and papillary thyroid carcinomas (n=3) that were negative for *RET* fusions by MSK-IMPACT and MSK-Fusion, and (iii) treatment-naïve papillary thyroid carcinomas (n=33) that were negative for *RET* SVs and positive for *BRAF* p.V600E by MSK-IMPACT. The last group was included given that *RET* fusions are mutually exclusive with the *BRAF* drivers in papillary thyroid carcinomas (34). Last, we included 10 cases that were negative for *RET* SVs on MSK-IMPACT but positive for high-level *RET* amplification as defined by >2 fold-change gain.

For each case, we performed a comprehensive semi-quantitative analysis capturing: (i) the staining intensity (1+, 2+, 3+), (ii) the estimated percentage of tumor cells with expression in 10% increments for each staining intensity, and (iii) the cellular localization of staining (e.g., membranous, cytoplasmic, and nuclear). Using the percentage and the staining intensity, we calculated the H-score for all cases as follows: (% with 1+) + 2 x (% with 2+) + 3 x (% with 3+). All cases were reviewed by a board-certified pathologist (SRY) blinded to the *RET* fusion results. Equivocal or borderline cases were reviewed independently and resolved by a second board-certified pathologist (JFH).

Data analysis

Statistical analyses were performed using R version 3.4.0 (R Project for Statistical Computing, Vienna, Austria) and GraphPad Prism version 8 (San Diego, California, USA). All tests of significance were two-tailed, and $P < 0.05$ was considered statistically significant. The 95% confidence intervals were calculated using exact binomial confidence limits. Publicly available data visualization tools were used for generating the circos plot(35) and the fusion proteins(36).

Results

Screening for *RET* fusions using DNA-based NGS

Of 46,897 tumors from 41,869 patients submitted for MSK-IMPACT, we detected *RET* structural variants (SVs) in 171 unique patient samples (0.4%), including 139 SVs that were predicted to result in oncogenic *RET* fusions with known partners and 32 SVs of uncertain significance (SVUS) (Figure 1a). Among the 139 *RET* SV predicted to be oncogenic, 105 cases were not further analyzed given the canonical nature of these fusions (group A). MSK-Fusion was performed in the remaining 34 cases, including 3 *RET* SVs that were reciprocal to known oncogenic fusions. On RNA sequencing, all 34 cases were confirmed to harbor *RET* fusion transcripts with the same partners as predicted by MSK-IMPACT (group B). In addition, MSK-Fusion was performed on all 32 cases with SVUS for further workup. In this

cohort, oncogenic *RET* fusion transcripts were detected in only 12 cases (group C) (37.5%), and the remaining 20 samples (62.5%) were negative for *RET* fusions (group D) (Supplementary Figure 1a). In all, we identified a total of 151 unique patient samples with oncogenic *RET* fusions (groups A, B, and C) using a combination of DNA and RNA-based sequencing (Figure 1b and 1c). The full clinical, pathologic, and molecular data are provided in Supplementary Table 1.

Group B cases

Here, we compared the oncogenic *RET* fusions that were predicted from DNA sequencing to the *RET* fusion transcripts that were detected on RNA sequencing in our group B cohort (n=34). For the 3 reciprocal SVs, we used the inferred pathogenic SV for our analysis. Despite sharing the same fusion partner, a total of 12 *RET* fusion transcripts (35.3%) showed exonic breakpoints that were slightly different from those predicted from DNA sequencing (Supplementary Table 1b). Specifically, 10 *RET* fusion transcripts had different breakpoints for the 5' fusion partner, with the majority of cases differing by a single exon (n=9, 90%). Only 3 *RET* fusion transcripts showed different 3' *RET* breakpoints as predicted from DNA sequencing, and most differed by a single *RET* exon (n=2, 66.7%). Furthermore, out-of-frame *RET* SVs were seen in 3 cases, and all had different 5' and/or 3' exonic breakpoints compared to the *RET* fusion transcripts detected on RNA sequencing.

Group C cases

While RNA sequencing detected *RET* kinase fusion transcripts in all group C cases (n=12), DNA sequencing identified only 5 *RET* SVs (41.7%) that were predicted to form a kinase fusion (3 in-frame and 2 mid-exon). In these 5 cases, the fusion partners and the exonic breakpoints predicted from DNA sequencing were identical to those identified on RNA sequencing. Among the 7 SVs not predicted to form a protein fusion, 4 (57.1%) involved rearrangements with intergenic regions, 2 (28.6%) were antisense fusions, and 1 (14.3%) was an intragenic *RET* deletion.

Group D cases

In this cohort of cases that lacked *RET* fusion transcripts (n=20), DNA sequencing predicted 5 *RET* protein fusions (25%), including 3 out-of-frame fusions, 1 mid-exon fusion, and 1 in-frame fusion. Among these, 1 SV was predicted to form a kinase fusion involving a 5' partner gene and a 3' *RET* kinase domain (*KCNMA1* exon 1 and *RET* exon 9-20); however, this was predicted to be out-of-frame. The remaining 4 fusions did not include the *RET* kinase domain in the 3' position and instead placed *RET* in the 5' location. Interestingly, these 5 partner genes are known to be widely expressed in many tissues, including their tissue of origin(37). While rearrangements involving these partner genes have been reported previously(38), they have not been seen in association with classic kinase partners (*ALK, ROS1, RET, NTRK1/2/3, EGFR*, and *MET*). The remaining 15 SVs (75%) in group D were not predicted to form a protein fusion; these included 3 antisense fusions, 2 of which were intragenic *RET* inversions, and 12 rearrangements involving intergenic regions.

Comparison of group C and D cases

In comparing groups C and D, SVUS that resulted in RNA-level fusions (group C) lacked concurrent driver alterations (0% vs. 60%, P = 0.0006, Fisher's exact test) and had higher normalized paired-end read support on MSK-IMPACT (0.059 vs. 0.018, P = 0.01, Mann–Whitney U test). Specifically, group C had a median and mean normalized paired-end read support of 0.059 and 0.084, respectively (range: 0.026-0.277) while group D had a median and mean normalized paired-end read support of 0.018 and 0.045, respectively (range: 0.002-0.182). In addition, group C cases were enriched in SVs predicted to form kinase fusions compared to group D (41.7% vs. 5%, P = 0.02, Fisher's exact test). To ensure that the fusion-negative results in group D were not due to low tumor purity or poor sample quality, we also compared the tumor cellularity and the cycle threshold values from MSK-Fusion between group D and group C cases and found no significant differences (P = 0.4 and P = 0.2, respectively, Mann–Whitney U test).

Clinical landscape of oncogenic *RET* fusions

Among our 151 patients with oncogenic *RET* fusions, the median age was 61 years (range: 3 months - 90 years), and the majority were women (n=93, 61.6%) (Table 1). The most common tumor type was non-small cell lung cancer (NSCLC) (n=99, 65.6%), followed by cancers from the thyroid (n=35, 23.2%), colorectum (n=7, 4.6%) and breast (n=3, 2%). The remaining tumors included 3 stomach adenocarcinomas (2%), a pancreatic adenocarcinoma (0.7%), an infantile fibrosarcoma (0.7%), a juvenile xanthogranuloma (0.7%), and a carcinoma of unknown primary (0.7%). Most patients had advanced stage tumors and lacked other activating MAPK alterations, supporting the oncogenic role of *RET* kinase fusions. In addition, nearly all tumors with non-*RET* driver alterations (83.3%, 5/6) came from patients who were previously treated with targeted or hormone therapies, thus implicating *RET* fusions as a potential resistance mechanism in these patients (39,40). Specifically, these included 4 lung cancer patients with activating *EGFR* mutations (2 exon 19 deletions and 2 L858R mutations) status post EGFR TKI therapy (range: 1-5 years) who acquired a *RUFY2-RET* fusion, a *NCOA4-RET* fusion and 2 *CCDC6-RET* fusions. There was also a patient with estrogen receptor positive breast cancer status post aromatase inhibitor therapy for 1 year who developed a *SPECC1L-RET* fusion. All of these patients showed clinical evidence of disease progression at the time of *RET* fusion detection. The clinicopathologic characteristics of group D patients are provided in Supplementary Table 2.

Prevalence of *RET* fusions in solid tumors

Given the diversity of tumors represented in our fusion-positive cohort, we analyzed the tumor-specific prevalence of *RET* fusions using our MSK-IMPACT database of 41,869 cases (Supplementary Table 3). Although *RET* fusions were rare in our unselected population (0.36%), they were enriched in patients with NSCLC (1.7%, 99/5,920) and thyroid cancer (4.9%, 35/710), as reported previously(41). Within thyroid cancers, papillary thyroid carcinomas showed the highest prevalence of *RET* fusions (7.8%, 27/348), followed by poorly differentiated thyroid carcinomas (4.7%, 7/148) and anaplastic thyroid carcinomas (1%, 1/98). In NSCLCs, *RET* fusions were identified in 2.1% (95/4,599) of lung

adenocarcinomas, 3% (3/101) of large cell neuroendocrine carcinomas, and 2% (1/49) of pleomorphic carcinomas. The remaining tumor subtypes had frequencies that were <1%.

Analysis of fusion partners

Among the 151 *RET* fusions, *KIF5B* was the most common partner (n=68, 45%), followed by *CCDC6* (n=44, 29.1%), and *NCOA4* (n=20, 13.3%) (Figure 1c). Other partners included *SPECC1L* (n=2), *CLIP1* (n=1), *TFG* (n=1), *EML4* (n=1), *C10orf118* (n=1), *RUFY1* (n=1), *RUFY2* (n=1), *RUFY3* (n=1), *KIF13A* (n=1), *TRIM24* (n=1), *ERC1* (n=1), *KIAA1468* (n=1), *KIAA1217* (n=1), *GEMIN5* (n=1), *SHROOM3* (n=1), *RBPMS* (n=1), *GRIPAP1* (n=1), and *MBIP* (n=1). The full clinical and molecular characteristics are summarized in Figure 2a.

Next, we analyzed the distribution of fusion partners with respect to tumor histology. In NSCLC, *KIF5B* was the most common partner (n=68, 68.7%) and not seen in other tumor types. Other variants included *CCDC6* (n=18, 18.2%), *NCOA4* (n=3, 3%), and other partners (n=10, 10.1%). In thyroid cancer, most of the fusions involved *CCDC6* (n=22, 62.9%), followed by *NCOA4* (n=9, 25.7%) and other partners (n=4, 11.4%). In the remaining tumors, *NCOA4* comprised nearly half of the fusions (n=8, 47%), while the rest were split between *CCDC6* (n=4, 24%) and other partners (n=5, 29%).

DNA-based NGS performance

While DNA-based NGS is being increasingly used to detect kinase fusions, its sensitivity and specificity for capturing *RET* fusions are not well characterized. Here, we evaluated the performance of MSK-IMPACT using MSK-Fusion as the reference standard (Table 2). In addition to the 66 samples (groups B, C, and D) that were co-tested with MSK-IMPACT and MSK-Fusion in our series, we surveyed an additional set of 4,459 tumors from our MSK-IMPACT database that were submitted for MSK-Fusion testing (See RNA sequencing under Materials and Methods). For this analysis, detection of a *RET* SV from MSK-IMPACT was considered *RET* positive. In this combined cohort of 4,525 cases that were co-tested with MSK-IMPACT and MSK-Fusion, MSK-IMPACT demonstrated 100% sensitivity (95% CI: 92.3-100%) and 99.6% specificity (95% CI: 99.3-99.7%) for detecting *RET* fusions. In particular, no new *RET* fusion transcripts were identified in the additional set of 4,459 tumors, and only 20 false-positive cases (group D) were present in the entire cohort. While the high specificity was maintained across the three different tumor groups, non-lung and non-thyroid malignancies comprised the majority of the false-positive cases (55%, 11/20). Notably, these false-positive SV calls had fewer read support on MSK-IMPACT compared to those that resulted in oncogenic fusion transcripts on MSK-Fusion (Figure 2b).

RET fusion detection using circulating tumor DNA

To explore the detection of *RET* fusions from circulating tumor cfDNA, we analyzed a subset of patients from our cohort (n=16) who underwent plasma-based cfDNA testing using MSK-ACCESS (Supplementary Table 1c). At the time of liquid biopsy, 2 patients had no evidence of disease (12.5%), whereas the remaining 14 patients had metastatic disease with no prior treatment (i.e., initial presentation) (n=3, 18.7%), progression of disease (n=5, 31.3%), ongoing response to treatment (n=1, 6.2%), and stable disease (n=5, 31.3%). In this

cohort of 16 patients, *RET* SVs were detected in 5 patients (31.3%) with either progression of disease (3/5, 60%) or at initial presentation (2/3, 66.7%). In 4 patients, cfDNA testing revealed the same *RET* SV as in tissue, with 2 cases sharing the identical genomic breakpoints and the remaining 2 cases showing slightly different genomic breakpoints but having the same exonic breakpoints as in tissue. These *RET* SVs included 2 oncogenic group A cases (*KIF5B-RET* and *KIF13A-RET*) and 2 group D cases with *RET* SVUS that were negative on tissue-based RNA sequencing. In the remaining case, liquid biopsy from a group D patient showed the same *RET* translocation with the identical genomic breakpoint as in tissue but with a different orientation.

Break-apart FISH performance

Next, we evaluated the sensitivity of break-apart FISH using a subset of our cases with *RET* fusions (n=48) and showed that sensitivity for FISH was 91.7% (95% CI: 80-97.7%) for detecting *RET* fusions (Table 2 and Figure 3). In this study, we did not include a large cohort of *RET* fusion-negative cases to determine overall specificity. Instead, our specificity analysis was mostly restricted to 8 cases from MSK-IMPACT that had *RET* SVs but no *RET* fusion transcripts on MSK-Fusion (i.e., group D cases that were false positive by MSK-IMPACT). Interestingly, all but one also showed a *RET* gene rearrangement (7/8) despite the lack of a *RET* fusion transcript, indicating that they are also false positive by FISH. Furthermore, the true positive and false positive cases did not show a difference in their median percentage of tumor cells with rearrangements (72.5% vs. 65%, P = 0.9, Mann–Whitney U test). Notably, most of the false positive cases (5/8) showed atypical rearrangements including loss of 5’ or 3’ signals, while only 2/48 of true *RET* fusion-positive cases demonstrated these atypical patterns (P = 0.003, Fisher’s exact test). In addition, we submitted 17 cases without *RET* SVs for FISH testing, and they were all negative for *RET* rearrangements.

Sensitivity of FISH by fusion partners

When stratified by fusion partners, FISH was 100% sensitive for both *KIF5B* (95% CI: 80.5-100%) and *CCDC6* (95% CI: 76.8-100%). However, *NCOA4* fusions were detected with a low sensitivity (66.7%, 95% CI: 34.9-90.1%) and showed a lower percentage of rearranged tumor cells compared to *KIF5B* and *CCDC6* fusions (P = 0.005, Mann–Whitney U test) (Figure 2b).

Sensitivity of FISH by tumor types

In addition to fusion partners, sensitivity varied among the three different tumor groups (P = 0.04), with NSCLC having high sensitivity (100%, 95% CI: 85.8-100%) followed by thyroid (87.5%, 95% CI: 61.7-98.4%) and the remaining tumor group (75%, 95% CI: 34.9-96.8%). This variation is likely driven by the different fractions of *NCOA4-RET* fusions in these groups given that *NCOA4* was seen in 4.2%, 37.5% and 62.5% of NSCLC, thyroid, and other tumors, respectively.

IHC performance

Last, we assessed the performance of RET IHC using 70 fusion-positive and 89 fusion-negative cases. Given that RET IHC is not routinely performed and its staining characteristics are not well established, we divided our cohort into a training (n=37, fusion-positive: 19, fusion-negative: 18) and validation set (n=122, fusion-positive: 51, fusion-negative: 71) to determine and to evaluate the optimal staining criteria, respectively. Data from the training set showed that cytoplasmic staining in ≥1% of tumor cells provided the most optimal cut-off point, with a sensitivity and specificity of 89.5% (17/19, 95% CI: 66.9-98.7%) and 88.9% (16/18, 95% CI: 65.3-98.6%), respectively. Using these criteria, the validation set showed a comparable sensitivity and specificity of 86.3% (44/51, 95% CI: 73.7-94.3%) and 80.3% (57/71, 95% CI: 69.1-88.8%), respectively. Combining the two cohorts together (n=159), the overall sensitivity and specificity were 87.1% (61/70, 95% CI: 77-93.9%) and 82% (73/89, 95% CI: 72.5-89.4%), respectively (Table 2).

IHC staining pattern

Among the *RET* fusion-positive cases (n=70), the tumor staining pattern was strikingly consistent, with nearly all expression being restricted to the cytoplasm as reported previously (8,24) (Figure 2c). One case, an infantile fibrosarcoma with a *SPECC1L-RET* fusion, had dual cytoplasmic and membranous staining. Among the *RET* fusion-positive cases, 9/70 (12.9%) lacked staining, 16/70 (22.9%) showed at most 1+ staining, 19/70 (27.1%) at most 2+ staining, and 26/70 (37.1%) at most 3+ staining. Among the *RET*-fusion negative cases (n=89), tumor cell staining was seen in 21 cases (23.6%) including 5 with membranous staining that was considered IHC negative. In addition, staining intensity in the fusion negative cohort was low, with most cases (12/21, 57.1%) showing only 1+ staining. Background staining in non-tumor cells included pneumocytes with apical-only staining and macrophages with globular cytoplasmic staining.

Sensitivity of IHC by fusion partner

Similar to FISH, sensitivity for IHC varied significantly with the different fusion partners ($P = 0.0003$, Fisher's exact test). Notably, IHC detected all *KIF5B* fusions (95% CI: 88.8-100%), and these fusions had higher H-scores compared to *CCDC6* ($P < 0.01$) and *NCOA4* ($P < 0.0001$) (Figure 2b). In contrast, IHC missed half of the *NCOA4* fusions (95% CI: 21.1-78.9%), and *NCOA4* fusions showed the lowest H-score among the fusion-positive cases.

Sensitivity and specificity of IHC by tumor type

Sensitivity also varied with tumor type ($P = 0.002$), with lung cancer showing the highest sensitivity (97.6%, 95% CI: 87.1-99.9%) followed by thyroid cancer (78.9%, 95% CI: 54.4%-93.9%) and other tumors (60%, 95% CI: 26.2-87.8%). Further, lung cancers showed higher H-scores compared to thyroid cancers ($P < 0.0001$) and other tumors ($P < 0.0001$). As expected, the sensitivity and H-scores appeared to be driven by the fraction of *NCOA4* cases: 2.4%, 31.6%, and 50% for NSCLC, thyroid, and other tumors, respectively. Specificity was consistently ≥80% for all three tumor types.

RET expression in *RET* amplified tumors

It is unclear if *RET* amplification is associated with RET overexpression in the absence of a *RET* fusion. To investigate, we included 10 tumors with *RET* amplification lacking *RET* SVs in our fusion-negative cases for IHC staining. These included 2 breast carcinomas, 2 uterine serous carcinomas, gastric carcinoma, melanoma, prostatic adenocarcinoma, uterine carcinosarcoma, ovarian carcinoma, and adenoid cystic carcinoma; majority of these tumors (60%) harbored disease-specific drivers (e.g., *TMPRSS2-ERG* in prostate and *ERBB2* amplification in breast). Among these, the 2 cases with the highest fold change (breast carcinoma and ovarian carcinoma with 7.6 and 5 fold change, respectively) showed strong IHC expression, indicating that high-level *RET* amplification may be associated with RET overexpression without a *RET* fusion. Interestingly, the staining pattern in these *RET*-amplified cases was unusually heterogeneous and distinct from fusion-mediated staining. Whereas fusion-positive cases showed a more uniform staining in large groups or sheets of cells, the *RET*-amplified cases presented with a more mosaic and checkered distribution.

RET inhibition in fusion-positive tumors with low or no RET expression

In tumors with *RET* fusions, RET TKI directly interacts with the chimeric RET oncoproteins to suppress tumor growth. Given the critical role of RET oncoproteins, we investigated whether RET targeted therapy remains active in a subset of fusion-positive tumors that lack robust RET expression by IHC (H-score <50). To do so, we selected 16 fusion-positive patients with H-score of <50 and identified only 4 patients who received selpercatinib in this cohort (Supplementary Table 4). The remaining patients (n=7) received standard treatments (e.g., surgery, radiation, chemotherapy, immunotherapy) while others (n=4) were treated with multikinase inhibitors (e.g., vandetanib, lenvatinib). One patient was lost to follow up. Among the 4 patients who received selpercatinib, 2 had low expression (NSCLC with H-score of 30 and papillary thyroid cancer with H-score of 10); while the remaining showed no expression (both papillary thyroid cancers with H-score of 0). Despite the lack of robust RET expression by IHC, all four patients with *RET* fusions showed responses to selpercatinib. While our finding suggests that RET targeted therapy remains active in fusion-positive tumors with low or no expression, this observation requires confirmation using a larger, prospective cohort.

Discussion

Given the approval of selpercatinib and pralsetinib, oncogenic *RET* fusions have emerged as a must-test biomarker in patients with advanced lung and thyroid cancers(22). In this study, we provide a comprehensive characterization of *RET* fusions and investigate the performance of various clinical-grade assays for detecting these highly actionable fusions.

By using a combination of DNA- and RNA-based NGS, we identified a large cohort of *RET* fusions across various tumor types. We confirm that the majority of *RET* fusions involve *KIF5B, CCDC6*, and *NCOA4* genes, all of which are located in chromosome 10 along with *RET* and demonstrate that their distribution varies with tissue type. Specifically, *KIF5B* fusions are exclusive to NSCLC, and *NCOA4* and *CCDC6* fusions are enriched in thyroid cancers. Interestingly, 19/151 (12.6%) *RET* fusions did not map to *KIF5B, CCDC6*, and

NCOA4, but instead were rearranged with a wide range of other partner genes. These less common 5' partner genes mostly mapped to other chromosomes including 2p21 (*EML4*), 3q12.2 (*TFG*), 4q13.3 (*RUFY3*), 4q21.1 (*SHROOM3*), 5q33.2 (*GEMIN5*), 5q35.3 (*RUFY1*), 6p22.3 (*KIF13A*), 7q33 (*TRIM24*), 8p12 (*RBPMS*), 12p13.33 (*ERC1*), 12q24.31 (*CLIP1*), 14q13.3 (*MBIP*), 18q21.33 (*KIAA1468*), 22q11.23 (*SPECC1L*), and Xp11.23 (*GRIPAP1*). Three partner genes mapped to the same chromosome as *RET* including *C10orf118* (10q25.3), *RUFY2* (10q21.3), and *KIAA1217* (10p12.2). Though uncommon, these non-classical fusions reveal the genetic diversity of *RET* fusions and underscore the need for diagnostic strategies that are partner-agnostic.

While our finding confirms that NSCLC and thyroid cancer comprise most tumors with *RET* fusions, we found similar fusions in other cancers lacking mitogenic drivers including *KRAS* wild-type pancreatic adenocarcinoma and *NTRK* wild-type infantile fibrosarcoma. Preliminary data have shown that RET targeted therapies may have pan-cancer activity(42), suggesting that *RET* fusions may serve as a tumor-agnostic biomarker. Furthermore, the presence of *RET* fusions in driver-positive tumors after targeted therapy adds to the growing evidence that *RET* fusions can facilitate drug resistance (15,43,44). Given that patients with acquired *RET* fusions are also sensitive to RET inhibition, screening for *RET* fusions in the post-treatment setting may be clinically meaningful (45). Taken together, our finding highlights the importance of *RET* fusion testing not only in lung and thyroid cancers but also in other driver-negative tumors and driver-positive tumors progressing on oncogene-directed therapies.

DNA-based sequencing is being increasingly used to detect *RET* fusions along with other molecular targets. However, its accuracy and performance for identifying *RET* fusions have not been rigorously evaluated despite its known limitations with fusions. In this study, we compared the results from our DNA-based MSK-IMPACT using our RNA-based MSK-Fusion as the reference. In our co-tested cohort with paired MSK-IMPACT and MSK-Fusion data, MSK-IMPACT detected *RET* SVs in all cases with *RET* fusion transcripts, highlighting its utility as a sensitive screening tool. The high sensitivity is likely due to the inclusion of probes targeting *RET* introns 7-11 and suggests that hybrid capture DNA-based NGS panels with similar intronic coverage may provide comparable sensitivity. Unlike introns in *NTRK3* or *NRG1, RET* intron tiling is more feasible as intron sequences are not as repetitive or long(46,47).

In our study, the majority of the *RET* SVs detected from DNA sequencing were predicted to form recurrent oncogenic *RET* fusions with previously characterized 5' partners (group A). A subset of these recurrent SVs was further analyzed by RNA sequencing (group B) and shown to have kinase fusion transcripts with the same fusion partner as predicted from DNA sequencing. Interestingly, in this group B cohort, a small number of DNA-level SVs and RNA-level fusion transcripts showed slight differences in their exonic breakpoints, with most cases differing by a single exon in the 5' fusion partner. This minor discordance in breakpoints may be due to alternative splicing, particularly for SVs that were predicted to form out-of-frame fusions. Given that these differences are small, uncommon, and seen mostly in the 5' fusion partner, the presence of these discordant breakpoints in classically oncogenic *RET* SVs is likely to be clinically insignificant.

Notably, MSK-IMPACT called a small group of *RET* SVs that were not confirmed as *RET* fusions on RNA sequencing (group D). These false positive cases were all SVs of unknown significance (SVUS), and most did not predict a *RET* kinase fusion. In fact, group D was enriched in SVs that were not predicted to form any protein fusions, including SVs with intergenic regions and antisense orientations. While there were 5 SVs predicted to form protein fusions in this cohort, only 1 was predicted to form a kinase fusion with a 5' partner gene and 3' *RET* kinase domain. The remaining 4 SVs contained *RET* exons in the 5' location and the non-*RET* partner genes in 3' position. Interestingly, a considerable number of similar SVUS (12/32, 37.5%) including those with intergenic and antisense rearrangements did result in *RET* kinase fusions (group C), arguing that RNA sequencing may be required for clarification in cases with SVUS (Figure 4a). While group C cases showed features that were more supportive of a potential oncogenic fusion (e.g., higher read support, absence of other mitogenic drivers, more SVs involving a 5' partner gene and a 3' *RET* kinase domain), these characteristics do not always correlate with the fusion status. As such, we recommend RNA sequencing for *RET* SVs with atypical or novel features.

Liquid biopsy using circulating tumor cell-free DNA (cfDNA) allows for non-invasive detection of actionable genetic variants including kinase fusions(15,48). Here, we demonstrate that *RET* SVs can be detected in a subset of patients using a plasma-based cfDNA NGS assay and that these *RET* SVs found in plasma correspond to those detected in tissue. In our small series, *RET* SVs were mostly identified in patients with metastatic tumors at initial presentation or during disease progression; none were identified in patients responding to therapy, with stable disease, or without disease. These findings suggest that *RET* fusion detection in plasma may vary with tumor load and treatment response, similar to the detection of other genetic variants using liquid biopsies(49). In addition to identifying canonical *RET* fusions such as *KIF5B-RET*, plasma testing also revealed *RET* SVUS that were not expressed on tissue RNA sequencing (group D). Hence, our findings suggest that liquid biopsy using circulating DNA can reveal both (i) classic *RET* fusions that are immediately actionable and (ii) atypical *RET* SVs that may require confirmatory RNA sequencing using tissue specimens.

FISH plays a critical role in fusion testing given its single-cell resolution and rapid turn-around time. As a screening strategy, it may be employed when DNA-based NGS is unavailable. Here, we show that break-apart FISH has modest sensitivity for most *RET* fusion partners but limited specificity. While FISH demonstrated high sensitivity for *KIF5B-RET* and *CCDC6-RET* fusions, it missed 33.3% (4/12) of *NCOA4-RET* fusions due to poor signal separation between the two probes. This finding is likely due to the close proximity of *NCOA4* (10q11.22) and *RET* (10q11.21) (Supplementary Figure 1b) and suggests that cases with subtle separation patterns should be confirmed using RNA-sequencing or an alternative FISH assay with an *NCOA4*-specific probe (Figure 4b) (50). In addition, nearly all false-positive cases on MSK-IMPACT (group D) were also false-positive by FISH, resulting in a false-positive rate of 28%. Although our study was not designed to evaluate for overall specificity, our findings are consistent with false-positive rates from prior studies (40-50%) (8,51) and highlight the potential pitfalls of relying exclusively on DNA-level events (FISH or DNA-based NGS). Given that these false-positive cases in our series were associated with

atypical loss of 5’ or 3’ signals, positive FISH results with unusual, complex patterns may benefit from further confirmation with RNA-sequencing.

Previous studies have explored the utility of RET IHC using small series of fusion-positive tumors. In all, these studies have reported a wide range of sensitivity (~50-100%) and specificity (~30-90%) (8,13,24,52–54) likely due to differences in clones, reference methods, and positivity thresholds. Here, we also explored the performance of RET IHC using a standard monoclonal RET antibody (EPR2871) but incorporated a few important updates. Unlike prior studies, we (1) set NGS as the composite gold standard (DNA NGS for canonical *RET* SVs and RNA NGS for all *RET* fusions), (2) divided the cohort into discovery and validation sets, (3) calculated H-scores to integrate both the intensity and the percentage of tumor staining, and (4) designed the study to evaluate for partner-specific expression. Through this approach, we show that while RET IHC has modest overall performance, expression varies significantly with the fusion partner, with *KIF5B-RET* showing diffuse and strong staining in most cases and *NCOA4-RET* lacking staining in half of the cases. Since prior studies using this clone have largely focused on *KIF5B-RET* fusions, our findings showing reduced staining in other fusion partners require further confirmation. In addition, future studies are needed to evaluate for partner-specific expression using other RET IHC clones.

The underlying mechanism for this partner-specific expression is unclear. Given that the fusion partners lie in the 5’ region, it is possible that potential differences in promoter activity and/or protein degradation signaling may be driving the variation in RET expression and stability. Interestingly, the fusion-positive tumors with reduced or absent RET IHC expression still responded to RET targeted therapy, suggesting that the RET oncoprotein was expressed and sensitive to inhibition. In this context, another potential mechanism could be accelerated decay of chimeric mRNA leading to lower expression of *RET* fusion transcripts. In clinical practice, RET IHC may be best suited for identifying lung cancers with *KIF5B-RET* fusions for pathologic diagnosis. However, due to the variability in expression for other *RET* fusions and tumor types, RET IHC has limited utility as a broad screening tool. For therapy selection, all RET IHC scores should be correlated with either FISH or NGS given that the clinical trials and approvals for RET targeted therapies were based on genetic testing results, not on IHC overexpression. Importantly, the absence of strong staining in fusion-positive tumors should not be used to withhold treatment given the responses seen in these patients.

For optimal detection of *RET* fusions, we recommend a testing strategy that incorporates both a screening and confirmation assay (Figure 4). First, we recommend DNA-based NGS, if available, as a primary screening tool given its broad sensitivity for all *RET* fusions. All exons and introns near the *RET* kinase domain should be covered. Detection of canonical *RET* SVs (e.g., *KIF5B-RET*) may be immediately actionable and not require further testing. Similarly, absence of *RET* SVs can be regarded as a negative result. However, any atypical *RET* SVUS with new fusion partners, intergenic regions, or antisense fusions should be further evaluated by RNA sequencing to evaluate for the presence of a *RET* fusion transcript. Dual up-front DNA and RNA sequencing may represent another option; however, it is unclear whether this approach is superior to sequential testing. If DNA-based NGS is

not available, we recommend screening with *RET* FISH. While a rearranged pattern can be regarded as a positive result, rearranged signals with atypical features may require further confirmation given the possibility of a false-positive result (group D cases). Similarly, while the absence of a clear rearranged pattern can be generally regarded as a negative result, a subthreshold split pattern may require further confirmation given the possibility of a false-negative result (e.g., *NCOA4-RET* fusions). As with DNA sequencing, we recommend RNA sequencing for confirmation of atypical positive and borderline-negative FISH results.

Our study has several limitations. First, our cohort was dominated by lung and thyroid cancer along with the three most common fusion isoforms (*KIF5B-RET, CCDC6-RET*, and *NCOA4-RET*). Given this bias, our findings may not be generalizable to fusions with other partner genes and those occurring in other tumors. Second, we did not use RNA sequencing to confirm the canonical *RET* fusions predicted by DNA sequencing. However, our results from group B confirm that these cases express fusion transcripts with the same fusion partner as predicted from DNA sequencing, indicating that RNA confirmation may not be necessary in these cases. Similarly, RNA sequencing was not consistently used to confirm the lack of *RET* fusions in our fusion-negative cases for FISH and IHC. To address this, we selected treatment-naïve tumors that were negative for *RET* SVs and positive for other mitogenic drivers on MSK-IMPACT to further minimize the possibility of selecting cases with occult *RET* fusions. Last, while our RNA sequencing assay was used as the gold standard, this assay targets only a portion of the *RET* transcript (exons 8-13). Though this region maps to a breakpoint hotspot, there is a possibility that rare *RET* kinase fusions with alternative breakpoints may be missed. Interestingly, we were able to detect a *CCDC6-RET* fusion with a breakpoint involving *RET* exon 2, suggesting that *RET* fusions with alternative breakpoints may still be captured using our targeted assay.

In summary, we present an integrated diagnostic atlas of oncogenic *RET* fusions by correlating their genomic, cytogenetic, and expression-based features. Our findings highlight the utility of RNA sequencing for confirming unusual *RET* rearrangements from DNA sequencing and FISH. In addition, our partner-specific analysis reveals limitations of FISH and IHC for certain fusion variants, particularly *NCOA4-RET*. Clinical application of these insights may improve the quality and accuracy of *RET* fusion testing.

Supplementary Material

Refer to Web version on PubMed Central for supplementary material.

Acknowledgements

This study was funded by the National Cancer Institute (NCI) under the MSK Cancer Center Support Grant/Core Grant (P30 CA008748) and by a research grant from Lilly Oncology (JFH).

Disclosure of Potential Conflicts of Interest:

SRY: Received consulting fees from Invitae.

RB: Received a grant and travel credit from ArcherDx, honoraria for advisory board participation from Loxo oncology and speaking fees from Illumina.

AD: Received fees from Loxo Oncology, a wholly owned subsidiary of Eli Lilly (honoraria), Blueprint (honoraria), Exelixis (honoraria), Ignyta/Genentech/Roche (honoraria/ad board), Bayer (honoraria/ad board), Takeda/Ariad/Millenium (honoraria/ad board), TP Therapeutics (honoraria/ad board), AstraZeneca (honoraria/ad board), Pfizer (honoraria/ad board), Helsinn (honoraria/ad board), BeiGene (honoraria/ad board), BerGenBio (honoraria/ad board), Hengrui (honoraria/ad board), Tyra (honoraria/ad board), Verastem (honoraria/ad board), MORE Health (honoraria/ad board), AbbVie (honoraria/ad board), 14ner/Elevation Oncology (honoraria/ad board/SAB), Remedica Ltd. (honoraria/ad board), ArcherDX (honoraria/ad board), and Monopteros (honoraria/ad board) and reports a patent for Pocket Oncology and UpToDate (Wolters Kluwer) with royalties paid from Wolters Kluwer, other from Merck (food/beverage), Puma (food/beverage), Merus (food/beverage), and Boehringer Ingelheim (food/beverage), and CME honoraria from Medscape, OncLive, PeerVoice, Physicians Education Resources, Targeted Oncology, Research to Practice, Axis, PeerView Institute, Paradigm Medical Communications, and WebMD.

ML: Received advisory board compensation from AstraZeneca, Bristol-Myers Squibb, Takeda, Lilly Oncology, Blueprint Medicines, and Bayer, and research support from LOXO Oncology and Helsinn Healthcare

JFH: Received research funding from Boehringer Ingelheim, Bayer, and Lilly Oncology and consulting fees and honoraria from WebMD, Illumina, Axiom Healthcare Strategies, Bayer, and Cor2Ed.

The remaining authors do not report any conflicts of interests.

References

1. Drilon A, Hu ZI, Lai GGY, Tan DSW. Targeting ret-driven cancers: Lessons from evolving preclinical and clinical landscapes [Internet]. Nat. Rev. Clin. Oncol Nature Publishing Group; 2018 [cited 2020 Aug 1]. page 151–67. Available from: https://pubmed.ncbi.nlm.nih.gov/29134959/ [PubMed: 29134959]
2. Takahashi M, Ritz J, Cooper GM. Activation of a novel human transforming gene, ret, by DNA rearrangement. Cell [Internet]. Cell; 1985 [cited 2020 Jul 16];42:581–8. Available from: https://pubmed.ncbi.nlm.nih.gov/2992805/ [PubMed: 2992805]
3. Arighi E, Borrello MG, Sariola H. RET tyrosine kinase signaling in development and cancer [Internet]. Cytokine Growth Factor Rev. Cytokine Growth Factor Rev; 2005 [cited 2020 Jul 16]. page 441–67. Available from: https://pubmed.ncbi.nlm.nih.gov/15982921/ [PubMed: 15982921]
4. Pierotti MA, Santoro M, Jenkins RB, Sozzi G, Bongarzone I, Grieco M, et al. Characterization of an inversion on the long arm of chromosome 10 juxtaposing D10S170 and RET and creating the oncogenic sequence RET/PTC. Proc Natl Acad Sci U S A [Internet]. National Academy of Sciences; 1992 [cited 2020 Jul 16];89:1616–20. Available from: /pmc/articles/PMC48503/?report=abstract [PubMed: 1542652]
5. Ju YS, Lee WC, Shin JY, Lee S, Bleazard T, Won JK, et al. A transforming KIF5B and RET gene fusion in lung adenocarcinoma revealed from whole-genome and transcriptome sequencing. Genome Res. Cold Spring Harbor Laboratory Press; 2012;22:436–45. [PubMed: 22194472]
6. Ou S-HI, Zhu VW. Catalog of 5′ fusion partners in RET+ NSCLC Circa 2020. JTO Clin Res Reports [Internet]. Elsevier BV; 2020 [cited 2020 Aug 1];1:100037. Available from: 10.1016/j.jtocrr.2020.100037
7. Collisson EA, Campbell JD, Brooks AN, Berger AH, Lee W, Chmielecki J, et al. Comprehensive molecular profiling of lung adenocarcinoma. Nature [Internet]. 2014 [cited 2017 Feb 19];511:543–50. Available from: 10.1038/nature13385 [PubMed: 25079552]
8. Tsuta K, Kohno T, Yoshida A, Shimada Y, Asamura H, Furuta K, et al. RET-rearranged non-small-cell lung carcinoma: A clinicopathological and molecular analysis. Br J Cancer. Nature Publishing Group; 2014;110:1571–8. [PubMed: 24504365]
9. Suehara Y, Arcila M, Wang L, Hasanovic A, Ang D, Ito T, et al. Identification of KIF5B-RET and GOPC-ROS1 fusions in lung adenocarcinomas through a comprehensive mRNA-based screen for tyrosine kinase fusions. Clin Cancer Res [Internet]. Clin Cancer Res; 2012 [cited 2020 Oct 20];18:6599–608. Available from: https://pubmed.ncbi.nlm.nih.gov/23052255/ [PubMed: 23052255]
10. Li AY, McCusker MG, Russo A, Scilla KA, Gittens A, Arensmeyer K, et al. RET fusions in solid tumors. Cancer Treat. Rev W.B. Saunders Ltd; 2019.
11. Weinreb I, Bishop JA, Chiosea SI, Seethala RR, Perez-Ordonez B, Zhang L, et al. Recurrent RET Gene Rearrangements in Intraductal Carcinomas of Salivary Gland. Am J Surg Pathol [Internet].

Lippincott Williams and Wilkins; 2018 [cited 2020 Jul 16];42:442–52. Available from: https://pubmed.ncbi.nlm.nih.gov/29443014/ [PubMed: 29443014]

12. Chou A, Brown IS, Kumarasinghe MP, Perren A, Riley D, Kim Y, et al. RET gene rearrangements occur in a subset of pancreatic acinar cell carcinomas. Mod Pathol [Internet]. Springer Nature; 2020 [cited 2020 Jul 16];33:657–64. Available from: https://pubmed.ncbi.nlm.nih.gov/31558784/ [PubMed: 31558784]
13. Wang R, Hu H, Pan Y, Li Y, Ye T, Li C, et al. RET fusions define a unique molecular and clinicopathologic subtype of non-small-cell lung cancer. J Clin Oncol. 2012;30:4352–9. [PubMed: 23150706]
14. Offin M, Guo R, Wu SL, Sabari J, Land JD, Ni A, et al. Immunophenotype and Response to Immunotherapy of RET -Rearranged Lung Cancers . JCO Precis Oncol [Internet]. American Society of Clinical Oncology (ASCO); 2019 [cited 2020 Jul 16];3:1–8. Available from: https://pubmed.ncbi.nlm.nih.gov/31192313/
15. Rich TA, Reckamp KL, Chae YK, Doebele RC, Iams WT, Oh M, et al. Analysis of cell-free DNA from 32,989 advanced cancers reveals novel co-occurring activating RET alterations and oncogenic signaling pathway aberrations. Clin Cancer Res [Internet]. American Association for Cancer Research Inc.; 2019 [cited 2020 Aug 1];25:5832–42. Available from: http://clincancerres.aacrjournals.org/ [PubMed: 31300450]
16. Drilon A, Wang L, Hasanovic A, Suehara Y, Lipson D, Stephens P, et al. Response to cabozantinib in patients with RET fusion-positive lung adenocarcinomas. Cancer Discov. American Association for Cancer Research; 2013;3:630–5. [PubMed: 23533264]
17. Subbiah V, Cote GJ. Advances in targeting RET-dependent cancers. Cancer Discov [Internet]. American Association for Cancer Research Inc.; 2020 [cited 2020 Aug 1];10:498–505. Available from: https://cancerdiscovery.aacrjournals.org/content/10/4/498 [PubMed: 32094155]
18. Subbiah V, Velcheti V, Tuch BB, Ebata K, Busaidy NL, Cabanillas ME, et al. Selective RET kinase inhibition for patients with RET-altered cancers. Ann Oncol [Internet]. 2018/06/19. 2018;29:1869–76. Available from: https://www.ncbi.nlm.nih.gov/pubmed/29912274 [PubMed: 29912274]
19. Drilon A, Oxnard G, Wirth L, Besse B, Gautschi O, Tan SWD, et al. PL02.08 Registrational Results of LIBRETTO-001: A Phase 1/2 Trial of LOXO-292 in Patients with RET Fusion-Positive Lung Cancers. J Thorac Oncol. Elsevier BV; 2019;14:S6–7.
20. Wirth L, Sherman E, Drilon A, Solomon B, Robinson B, Lorch J, et al. LBA93Registrational results of LOXO-292 in patients with RET-altered thyroid cancers. Ann Oncol. 2019;30.
21. Gainor JF, Curigliano G, Kim D-W, Lee DH, Besse B, Baik CS, et al. Registrational dataset from the phase I/II ARROW trial of pralsetinib (BLU-667) in patients (pts) with advanced RET fusion+ non-small cell lung cancer (NSCLC). J Clin Oncol. American Society of Clinical Oncology (ASCO); 2020;38:9515–9515.
22. Markham A Selpercatinib: First Approval. Drugs [Internet]. Adis; 2020 [cited 2020 Aug 2];80:1119–24. Available from: 10.1007/s40265-020-01343-7 [PubMed: 32557397]
23. Go H, Jung YJ, Kang HW, Park IK, Kang CH, Lee JW, et al. Diagnostic method for the detection of KIF5B-RET transformation in lung adenocarcinoma. Lung Cancer [Internet]. Lung Cancer; 2013 [cited 2020 Jul 16];82:44–50. Available from: https://pubmed.ncbi.nlm.nih.gov/23932363/ [PubMed: 23932363]
24. Sasaki H, Shimizu S, Tani Y, Maekawa M, Okuda K, Yokota K, et al. RET expression and detection of KIF5B/RET gene rearrangements in Japanese lung cancer. Cancer Med [Internet]. Blackwell Publishing Ltd; 2012 [cited 2020 Jul 16];1:68–75. Available from: https://pubmed.ncbi.nlm.nih.gov/23342255/ [PubMed: 23342255]
25. Drilon A, Somwar R, Mangatt BP, Edgren H, Desmeules P, Ruusulehto A, et al. Response to ERBB3-directed targeted therapy in NRG1 -rearranged cancers. Cancer Discov [Internet]. American Association for Cancer Research Inc.; 2018 [cited 2020 Mar 1];8:686–95. Available from: http://www.ncbi.nlm.nih.gov/pubmed/29610121 [PubMed: 29610121]
26. Davies KD, Le AT, Sheren J, Nijmeh H, Gowan K, Jones KL, et al. Comparison of Molecular Testing Modalities for Detection of ROS1 Rearrangements in a Cohort of Positive Patient Samples. J Thorac Oncol [Internet]. Elsevier Inc; 2018 [cited 2020 Aug 1];13:1474–82. Available from: 10.1016/j.jtho.2018.05.041 [PubMed: 29935306]

27. Cohen D, Hondelink LM, Solleveld-Westerink N, Uljee SM, Ruano D, Cleton-Jansen AM, et al. Optimizing Mutation and Fusion Detection in NSCLC by Sequential DNA and RNA Sequencing. J Thorac Oncol. Elsevier Inc; 2020;15:1000–14. [PubMed: 32014610]
28. Benayed R, Offin M, Mullaney K, Sukhadia P, Rios K, Desmeules P, et al. High yield of RNA sequencing for targetable kinase fusions in lung adenocarcinomas with no mitogenic driver alteration detected by DNA sequencing and low tumor mutation burden. Clin Cancer Res [Internet]. American Association for Cancer Research Inc.; 2019 [cited 2020 Jul 16];25:4712–22. Available from: https://pubmed.ncbi.nlm.nih.gov/31028088/ [PubMed: 31028088]
29. Zehir A, Benayed R, Shah RH, Syed A, Middha S, Kim HR, et al. Mutational landscape of metastatic cancer revealed from prospective clinical sequencing of 10,000 patients. Nat Med. Nature Publishing Group; 2017;23:703–13. [PubMed: 28481359]
30. Rausch T, Zichner T, Schlattl A, Stütz A, Benes V, Korbel J. DELLY: Structural variant discovery by integrated paired-end and split-read analysis. Bioinformatics. 2012;28:i333–9. [PubMed: 22962449]
31. Rose Brannon A, Jayakumaran G, Diosdado M, Patel J, Razumova A, Hu Y, et al. Enhanced specificity of high sensitivity somatic variant profiling in cell-free DNA via paired normal sequencing: design, validation, and clinical experience of the MSK-ACCESS liquid biopsy assay. bioRxiv [Internet]. Cold Spring Harbor Laboratory; 2020 [cited 2020 Oct 20];2020.06.27.175471. Available from: 10.1101/2020.06.27.175471
32. Chen X, Schulz-Trieglaff O, Shaw R, Barnes B, Schlesinger F, Källberg M, et al. Manta: Rapid detection of structural variants and indels for germline and cancer sequencing applications. Bioinformatics [Internet]. Oxford University Press; 2016 [cited 2020 Oct 20];32:1220–2. Available from: https://pubmed.ncbi.nlm.nih.gov/26647377/ [PubMed: 26647377]
33. Zheng Z, Liebers M, Zhelyazkova B, Cao Y, Panditi D, Lynch KD, et al. Anchored multiplex PCR for targeted next-generation sequencing. Nat Med [Internet]. Nature Publishing Group; 2014 [cited 2020 Oct 20];20:1479–84. Available from: https://pubmed.ncbi.nlm.nih.gov/25384085/ [PubMed: 25384085]
34. Agrawal N, Akbani R, Aksoy BA, Ally A, Arachchi H, Asa SL, et al. Integrated Genomic Characterization of Papillary Thyroid Carcinoma. Cell [Internet]. Cell Press; 2014 [cited 2020 Jul 16];159:676–90. Available from: https://pubmed.ncbi.nlm.nih.gov/25417114/ [PubMed: 25417114]
35. Yu Y, Ouyang Y, Yao W. ShinyCircos: An R/Shiny application for interactive creation of Circos plot. Bioinformatics [Internet]. Oxford University Press; 2018 [cited 2020 Aug 15];34:1229–31. Available from: https://europepmc.org/article/med/29186362 [PubMed: 29186362]
36. Zhou X, Edmonson MN, Wilkinson MR, Patel A, Wu G, Liu Y, et al. Exploring genomic alteration in pediatric cancer using ProteinPaint [Internet]. Nat. Genet Nature Publishing Group; 2015 [cited 2020 Aug 15]. page 4–6. Available from: https://www.nature.com/articles/ng.3466
37. Uhlen M, Zhang C, Lee S, Sjöstedt E, Fagerberg L, Bidkhori G, et al. A pathology atlas of the human cancer transcriptome. Science (80-) [Internet]. American Association for the Advancement of Science; 2017 [cited 2020 Oct 20];357. Available from: https://pubmed.ncbi.nlm.nih.gov/28818916/
38. Kim P, Zhou X. FusionGDB: Fusion gene annotation DataBase. Nucleic Acids Res [Internet]. Oxford University Press; 2019 [cited 2020 Oct 20];47:D994–1004. Available from: https://pubmed.ncbi.nlm.nih.gov/30407583/ [PubMed: 30407583]
39. Offin M, Somwar R, Rekhtman N, Benayed R, Chang JC, Plodkowski A, et al. Acquired ALK and RET Gene Fusions as Mechanisms of Resistance to Osimertinib in EGFR -Mutant Lung Cancers . JCO Precis Oncol. American Society of Clinical Oncology (ASCO); 2018;2:1–12. [PubMed: 30949620]
40. Ross DS, Liu B, Schram AM, Razavi P, Lagana SM, Zhang Y, et al. Enrichment of kinase fusions in ESR1 wild-type, metastatic breast cancer revealed by a systematic analysis of 4854 patients. Ann Oncol [Internet]. Elsevier Ltd; 2020 [cited 2020 Oct 20];31:991–1000. Available from: https://pubmed.ncbi.nlm.nih.gov/32348852/ [PubMed: 32348852]
41. Li AY, McCusker MG, Russo A, Scilla KA, Gittens A, Arensmeyer K, et al. RET fusions in solid tumors [Internet]. Cancer Treat. Rev W.B. Saunders Ltd; 2019 [cited 2020 Jul 16]. Available from: https://pubmed.ncbi.nlm.nih.gov/31715421/

42. Subbiah V, Hu MI-N, Gainor JF, Mansfield AS, Alonso G, Taylor MH, et al. Clinical activity of the RET inhibitor pralsetinib (BLU-667) in patients with RET fusion+ solid tumors. J Clin Oncol. American Society of Clinical Oncology (ASCO); 2020;38:109–109.
43. McCoach CE, Le AT, Gowan K, Jones K, Schubert L, Doak A, et al. Resistance mechanisms to targeted therapies in ROS1þ and ALKþ non–small cell lung cancer. Clin Cancer Res [Internet]. American Association for Cancer Research Inc.; 2018 [cited 2020 Aug 3];24:3334–47. Available from: https://pubmed.ncbi.nlm.nih.gov/29636358/ [PubMed: 29636358]
44. Klempner SJ, Bazhenova LA, Braiteh FS, Nikolinakos PG, Gowen K, Cervantes CM, et al. Emergence of RET rearrangement co-existing with activated EGFR mutation in EGFR-mutated NSCLC patients who had progressed on first- or second-generation EGFR TKI. Lung Cancer [Internet]. Elsevier Ireland Ltd; 2015 [cited 2020 Aug 3];89:357–9. Available from: https://pubmed.ncbi.nlm.nih.gov/26187428/ [PubMed: 26187428]
45. Piotrowska Z, Isozaki H, Lennerz JK, Gainor JF, Lennes IT, Zhu VW, et al. Landscape of acquired resistance to osimertinib in EGFR-mutant NSCLC and clinical validation of combined EGFR and RET inhibition with osimertinib and BLU-667 for acquired RET fusion. Cancer Discov [Internet]. American Association for Cancer Research Inc.; 2018 [cited 2020 Jul 16];8:1529–39. Available from: https://pubmed.ncbi.nlm.nih.gov/30257958/ [PubMed: 30257958]
46. Nagasaka M, Ou SHI. Neuregulin 1 Fusion–Positive NSCLC. J Thorac Oncol. Elsevier Inc; 2019;14:1354–9. [PubMed: 31128291]
47. Solomon JP, Linkov I, Rosado A, Mullaney K, Rosen EY, Frosina D, et al. NTRK fusion detection across multiple assays and 33,997 cases: diagnostic implications and pitfalls. Mod Pathol [Internet]. Springer Nature; 2020 [cited 2020 Oct 20];33:38–46. Available from: https://pubmed.ncbi.nlm.nih.gov/31375766/ [PubMed: 31375766]
48. McCoach CE, Blakely CM, Banks KC, Levy B, Chue BM, Raymond VM, et al. Clinical utility of cell-free DNA for the detection of ALK fusions and genomic mechanisms of ALK inhibitor resistance in non–small cell lung cancer. Clin Cancer Res [Internet]. American Association for Cancer Research Inc.; 2018 [cited 2020 Oct 20];24:2758–70. Available from: https://pubmed.ncbi.nlm.nih.gov/29599410/ [PubMed: 29599410]
49. Wan JCM, Massie C, Garcia-Corbacho J, Mouliere F, Brenton JD, Caldas C, et al. Liquid biopsies come of age: Towards implementation of circulating tumour DNA. Nat. Rev. Cancer. Nature Publishing Group; 2017. page 223–38. [PubMed: 28233803]
50. Zhang T, Lu Y, Ye Q, Zhang M, Zheng L, Yin X, et al. An evaluation and recommendation of the optimal methodologies to detect RET gene rearrangements in papillary thyroid carcinoma. Genes Chromosom Cancer [Internet]. Blackwell Publishing Inc.; 2015 [cited 2020 Jul 16];54:168–76. Available from: https://pubmed.ncbi.nlm.nih.gov/25407564/ [PubMed: 25407564]
51. Takeuchi K, Soda M, Togashi Y, Suzuki R, Sakata S, Hatano S, et al. RET, ROS1 and ALK fusions in lung cancer. Nat Med [Internet]. 2012 [cited 2017 Mar 9];18:378–81. Available from: http://www.ncbi.nlm.nih.gov/pubmed/22327623 [PubMed: 22327623]
52. Lee SE, Lee B, Hong M, Song JY, Jung K, Lira ME, et al. Comprehensive analysis of RET and ROS1 rearrangement in lung adenocarcinoma. Mod Pathol. Nature Publishing Group; 2015;28:468–79. [PubMed: 25234288]
53. Lipson D, Capelletti M, Yelensky R, Otto G, Parker A, Jarosz M, et al. Identification of new ALK and RET gene fusions from colorectal and lung cancer biopsies. Nat Med [Internet]. NIH Public Access; 2012 [cited 2020 Jul 16];18:382–4. Available from: /pmc/articles/PMC3916180/?report=abstract [PubMed: 22327622]
54. Platt A, Morten J, Ji Q, Elvin P, Womack C, Su X, et al. A retrospective analysis of RET translocation, gene copy number gain and expression in NSCLC patients treated with vandetanib in four randomized Phase III studies. BMC Cancer [Internet]. BioMed Central Ltd.; 2015 [cited 2020 Jul 16];15:171. Available from: 10.1186/s12885-015-1146-8 [PubMed: 25881079]

Translational Relevance

RET fusions are oncogenic drivers that predict sensitivity to RET targeted therapies. Given the FDA-approval of the selective RET inhibitors selpercatinib and pralsetinib, *RET* fusion testing is now required to administer the standard of care for patients with advanced lung and thyroid cancer. However, the current diagnostic landscape is complicated by the use of different methods with variable performance characteristics. In this study, we compare three assays (NGS, FISH, and IHC) and evaluate their diagnostic utility in a large pan-cancer cohort. By using a combination of DNA, RNA, and protein-based methods, we present a comprehensive characterization of oncogenic *RET* fusions, and in doing so, reveal new patterns that have direct implications for clinical testing and treatment. Our findings suggest practical solutions and potential strategies for standardizing *RET* fusion testing.

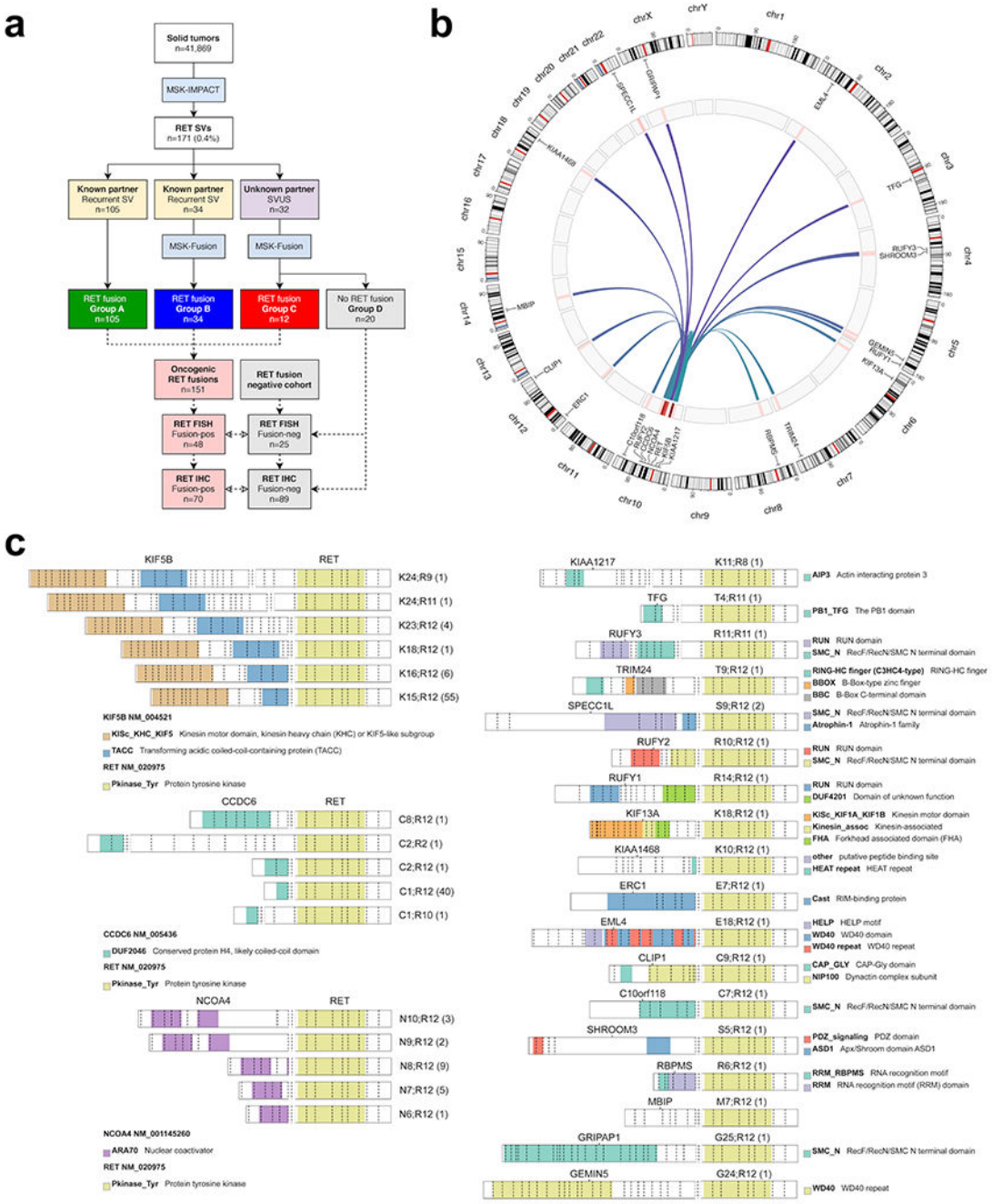

Figure 1: Oncogenic *RET* fusions

(A) Solid tumors were screened for *RET* fusions using a targeted DNA-based NGS assay (MSK-IMPACT). A subset of recurrent oncogenic *RET* structural variants (SVs) and all *RET* structural variants of unknown significance (SVUS) were confirmed using a targeted RNA-based NGS panel (MSK-Fusion). Through this approach, a total of 151 oncogenic *RET* fusions were identified. A subset of these fusions was further tested by break-apart FISH and immunohistochemistry (IHC). (B) Distribution of oncogenic *RET* fusions (n=151) across the genome. Red bars indicate frequency for each fusion type. (C) Distribution of

RET fusions involving *KIF5B, CCDC6*, and *NCOA4* partners (left panel) and other rare fusion partners (right panel). The exonic breakpoints and the observed frequency (in parenthesis) are provided for each fusion. The colors correspond to different protein domains.

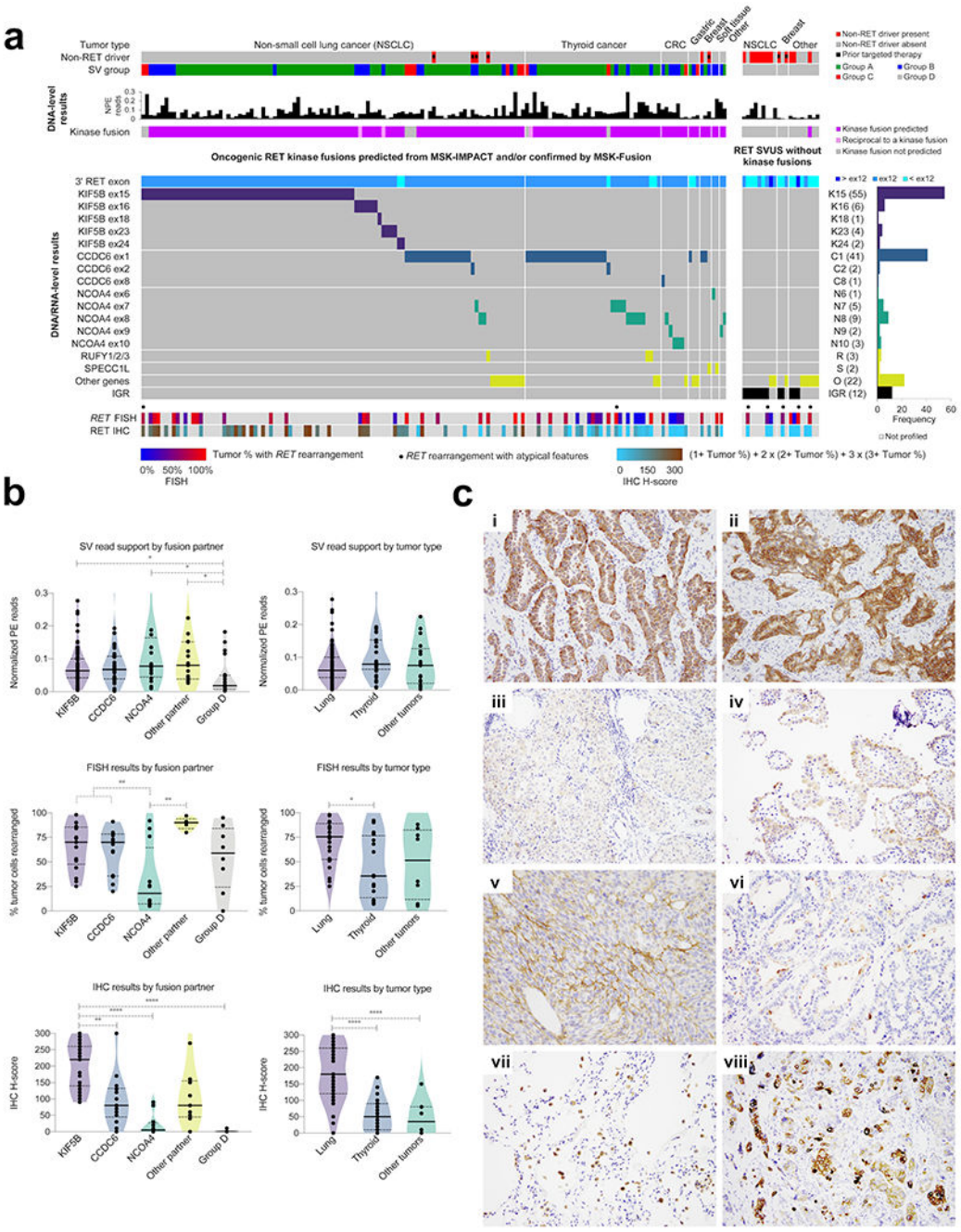

Figure 2: Comprehensive characterization of oncogenic *RET* fusions

(A) Clinical and molecular characteristics of oncogenic *RET* fusions (left panel) and *RET* SVUS that were negative for *RET* fusions (group D cases) (right panel). Top panel depicts the tumor type, non-*RET* driver status, and structural variant group (e.g., groups A, B, C, and D). DNA-level results are provided from MSK-IMPACT only. The *RET* breakpoints and the partner genes are shown using a composite dataset from MSK-IMPACT (groups A and D) and MSK-Fusion (groups B and C). The bottom panels describe the results from *RET* FISH and RET IHC. SV=Structural variant; NPE=Normalized paired-end reads; K=*KIF5B*;

C=*CCDC6*; N=*NCOA4*; R=*RUFY1/2/3*; S=*SPECC1L*; O=Other genes; IGR=Intergenic region. (B) Analysis by fusion partner and tumor types. Top panels: Paired-end (PE) read support for *RET* structural variants as detected by MSK-IMPACT. The number of reads were normalized by the median depth of sequencing for each sample. Middle panels: Percentage of tumor cells with *RET* rearrangements from break-apart FISH. Bottom panels: RET immunohistochemistry (IHC) H-scores. The median and the quartiles (25% and 75%) are represented by the solid and the dotted lines, respectively. Kruskal-Wallis test (with the post-hoc Dunn's test) was performed; only the statistically significant ($P < 0.05$) comparisons are highlighted. *P <0.05, **P <0.01, ***P < 0.001, ****P < 0.0001. (C) RET immunohistochemistry. (i, ii) *KIF5B-RET* lung adenocarcinoma with diffuse, 2-3+ cytoplasmic staining. (iii) *NCOA4-RET* and (iv) *CCDC6-RET* papillary thyroid cancer with patchy 1-2+ cytoplasmic staining. (v) *SPECC1L-RET* infantile fibrosarcoma with dual cytoplasmic and membranous staining. (vi) Lung adenocarcinoma negative for *RET* fusion with patchy, 2-3+ apical and membranous but not cytoplasmic staining. (vii) Lung parenchyma with 3+ staining of normal alveolar macrophages and some normal pneumocytes. (viii) *RET*-amplified tumor with heterogeneous and mosaic staining pattern. *RET* SV was not present.

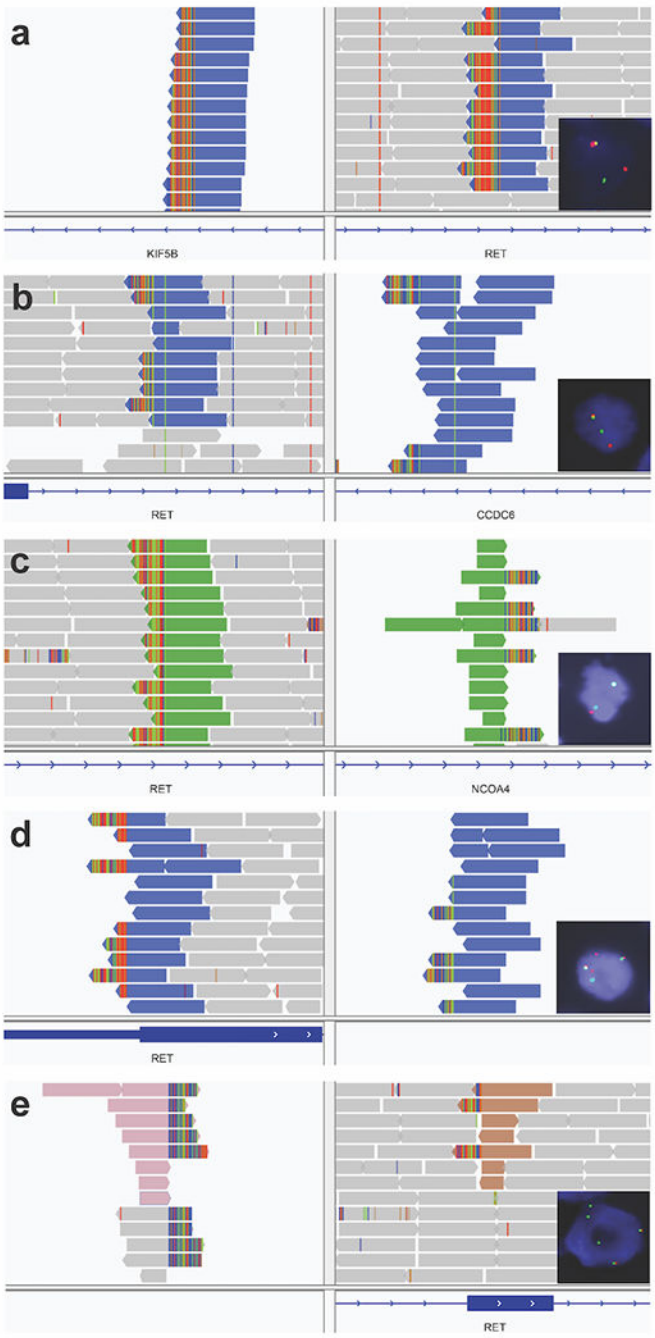

Figure 3: *RET* structural variants on DNA sequencing and rearrangements on FISH

(A) Lung adenocarcinoma (group B) with a *KIF5B-RET* structural variant (SV). FISH showed a *RET* rearrangement in 44% of tumor cells. RNA sequencing showed a *KIF5B-RET* fusion. (B) Anaplastic thyroid carcinoma (group A) with *CCDC6-RET* SV. FISH showed a *RET* rearrangement in 68% of tumor cells. RNA sequencing was not performed. (C) Papillary thyroid carcinoma (group A) with *NCOA4-RET* SV. FISH showed a subtle split pattern that was not considered rearranged. RNA sequencing was not performed. (D) Pancreatic adenocarcinoma (group D) with an inversion connecting an intergenic region (91

Kb before *LINC01468*) to intron 3 in *RET*. FISH showed a *RET* rearrangement in 95% of tumor cells. RNA sequencing did not show a *RET* fusion. (E) Invasive breast cancer (group D) with a translocation connecting an intergenic region (9178 Kb before *PREP*) to exon 9 in *RET*. FISH showed a *RET* rearrangement in 53% of tumor cells with loss of 5' signal (red). RNA sequencing did not show a *RET* fusion.

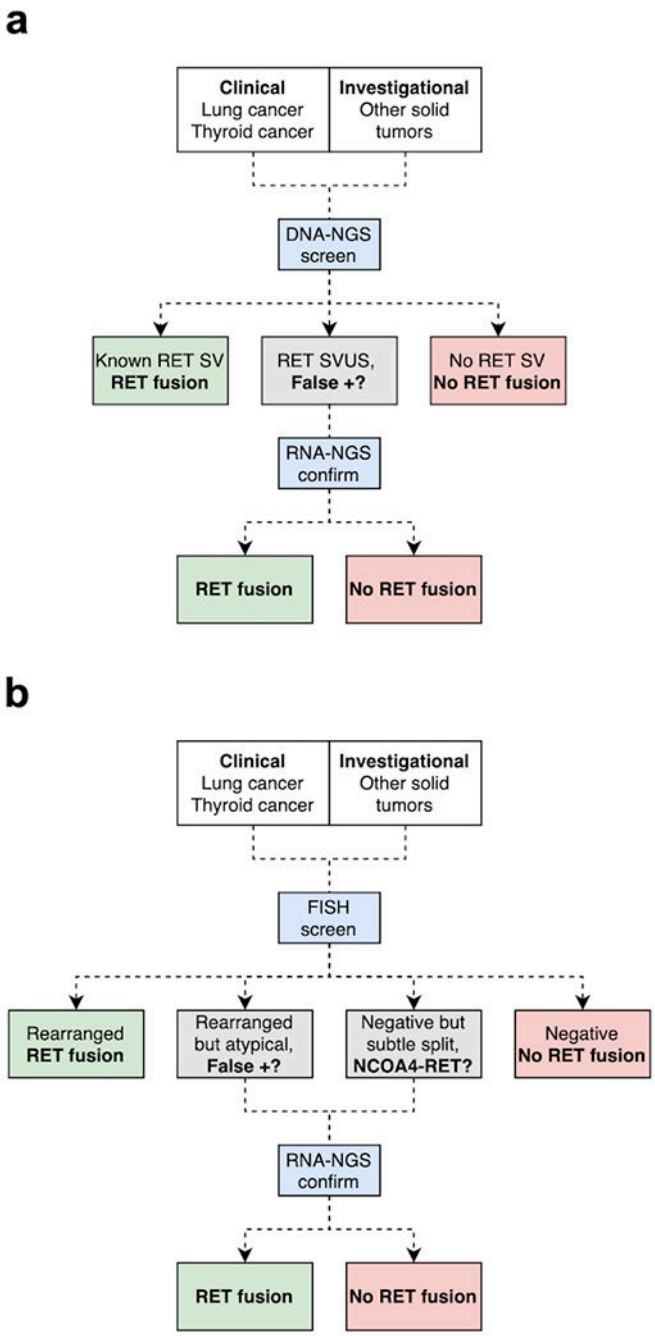

Figure 4: Proposed algorithm for *RET* fusion detection

(A) Screening using DNA-based NGS and confirmation using RNA-based NGS. (B) Screening using break-apart FISH and confirmation using RNA-based NGS when DNA-based NGS is not available. DNA-based NGS is preferable to FISH as a screen due to higher sensitivity for *NCOA4-RET* fusions. While *RET* fusion testing is clinically indicated for advanced lung and thyroid cancers, testing for other solid tumors may be considered to support ongoing clinical trials exploring pan-cancer indications.

Table 1:

Clinicopathologic and molecular characteristics of patients with oncogenic *RET* fusions

	Patients with oncogenic *RET* fusions (n=151)
Age	
Median	61 years
Range	3 months - 90 years
Sex	
Female	93 (61.6%)
Male	58 (38.4%)
Tumor type	
NSCLC	99 (65.6%)
Thyroid	35 (23.2%)
Colorectal	7 (4.6%)
Breast	3 (2%)
Other	7 (4.6%)
Stage	
I-III	36 (23.8%)
IV	113 (74.8%)
N/A	2 (1.3%)
Non-*RET* drivers[1]	
Absent	145 (96%)
Present[2]	6 (4%)
Fusion partners	
KIF5B	68 (45%)
CCDC6	44 (29.1%)
NCOA4	20 (13.3%)
Other	19 (12.6%)

[1]Non-*RET* oncogenic drivers include activating MAPK alterations (e.g., *EGFR* exon 19 deletion, *ERBB2* amplification) and hormone overexpression in breast cancers.

[2]History of prior targeted and hormone therapy was identified in 5/6 patients with non-*RET* oncogenic drivers. Abbreviations: NSCLC=Non-small cell lung cancer; N/A=Not available.

Table 2:

Performance of MSK-IMPACT, FISH, and IHC

	MSK-IMPACT[1]		*RET* FISH[2]		RET IHC[2]	
	Sensitivity	**Specificity**	**Sensitivity**	**Specificity[3]**	**Sensitivity**	**Specificity**
Total	100% 92.3-100% (46/46)	99.6% 99.3-99.7% (4459/4479)	91.7% 80-97.7% (44/48)	72% 50.6-87.9% (18/25)	87.1% 77-93.9% (61/70)	82% 72.5-89.4% (73/89)
Partners						
KIF5B	100% 78.2-100% (15/15)	N/A	100% 80.5-100% (17/17)	N/A	100% 88.8-100% (31/31)	N/A
CCDC6	100% 73.5-100% (12/12)	N/A	100% 76.8-100% (14/14)	N/A	88.9% 65.3-98.6% (16/18)	N/A
NCOA4	100% 63.1-100% (8/8)	N/A	66.7% 34.9-90.1% (8/12)	N/A	50% 21.1-78.9% (6/12)	N/A
Other	100% 71.5-100% (11/11)	N/A	100% 47.8-100% (5/5)	N/A	88.9% 51.8-99.7% (8/9)	N/A
Tumor						
Lung	100% 87.2-100% (27/27)	99% 98.1-99.5% (866/875)	100% 85.8-100% (24/24)	85% 62.1-96.8% (17/20)	97.6% 87.1-99.9% (40/41)	83.8% 68-93.8% (31/37)
Thyroid	100% 59-100% (7/7)	100% 95.8-100% (86/86)	87.5% 61.7-98.4% (14/16)	N/A	78.9% 54.4%-93.9% (15/19)	80.6% 64-91.8% (29/36)
Other	100% 73.5-100% (12/12)	99.7% 99.4-99.8% (3507/3518)	75% 34.9-96.8% (6/8)	20% 0.5-71.6% (1/5)	60% 26.2-87.8% (6/10)	81.3% 54.4-96% (13/16)

[1]The performance of MSK-IMPACT was analyzed using MSK-Fusion as the reference.

[2]The performance of IHC and FISH was analyzed using a composite reference of MSK-Fusion and MSK-IMPACT (canonical SVs only).

[3]Overall specificity was not evaluated for FISH. The provided specificity analysis was mainly to assess for *RET* rearrangements in group D cases.
N/A=Not applicable.